Available online at www.sciencedirect.com

ScienceDirect

Physics Procedia 14 (2011) 139–142

Physics Procedia

9th International Conference on Nano-Molecular Electronics

DFT study on the interaction of Fullerene (C_{60}) with hydroxyl radical (OH)

Hiroto TACHIKAWA,[a],1* Tetsuji IYAMA[a] and Shigeaki ABE[b]

[a]*Division of Materials Chemistry, Graduate School of Engineering, Hokkaido University, Sapporo 060-8628, JAPAN*

[b]*Department of Biomedical Materials and Engineering, Graduate School of Dental Medicine, Hokkaido University, North 13, West 7, Kita-ku, Sapporo 060-8586, Japan*

Abstract

The interaction of OH radical with C_{60} has been investigated by means of DFT method in order to elucidate the radical scavenge mechanism of fullerene. The OH radical was examined as an organic radical because the radical has a high reactivity. The DFT calculation showed that the OH radical binds to the carbon atom of C_{60} and a strong C-O bond is formed. The binding energies were calculated to be 36.4 and 35.2 kcal/mol at the B3LYP/6-31G(d) and 6-311G(d,p) levels of theory. The potential energy curve plotted as a function of C-O distance showed that the OH radical approaches to the carbon atom without activation barrier. Also, it was found that structural change from sp^2 to sp^3-like hybridization occurs easily by the approach of OH. The unpaired electron is distributed widely over the C_{60} surface in the C_{60}(OH) complex..

Keywords: fullerence; radical; scavenger; DFT; potential energy curve

1. Introduction

Fullerene has some potential biological effects, e.g. inhibition of HIV protease, antiviral activity, specific cleavage of DNA and photodynamic therapy [1], which has attracted considerable attention and has become a challenging research field. However, the fullerene is not soluble in water. The fullerol of C_{60}, hydroxyl radical is added to C_{60}, is one of the water-soluble fullerene derivatives to be suitable for biological study.

Electron spin resonance (ESR) spectroscopy and spin-trapping technique have proved that fullerol of C_{60} can efficient scavenge active oxygen radicals such as superoxide radical (O_2^-) [2] and hydroxyl radical (OH) [3]. Using time-resolved technique of laser photolysis, Lu et al. found that fullerol of C_{60} exists in aqueous solution and fullerol

* Corresponding author. Tel.: +81-11-706-6750; fax: +81-11-706-7897.
E-mail address: hiroto@eng.hokudai.ac.jp.

1875-3892 © 2011 Published by Elsevier Ltd. Open access under CC BY-NC-ND license.
doi:10.1016/j.phpro.2011.05.027

of C_{60} reacts with the primary irradiated products of water radiolysis [4]. Zeynalov investigated to determine the rate constants for addition of radicals to fullerenes [5].

In the present study, density functional theory (DFT) method is applied to the interaction system of C_{60} with hydroxyl radical (OH). The reaction of radical addition to C_{60} is investigated using potential energy calculation.

2. Method of calculation

The C_{60} fullerene molecule and hydroxyl radical (OH) were examined as a fullerene and radical, respectively. The structures of fullerene C_{60} and OH radical adduct, C_{60}(OH), were fully optimized at the B3LYP/6-31G(d) and UB3LYP/6-31G(d) levels of theory, respectively. The atomic charges were calculated using the natural bond population analysis (NPA) method at the B3LYP/6-31G(d) level. For comparison, M06 exchange correlation functional was used for the calculation of potential energy curve.

The excitation energies were calculated by means of time dependent (TD) DFT method, UB3LYP/6-31G(d), while ten states were solved for the excited states. All density functional theory (DFT) calculations were carried out using Gaussian 03 program package [6]. Previous studies showed that this level of theory give a reasonable electronic structure of carbon systems [7-11]. Electron spin operator $<S^2>$ values of C_{60}(OH) were less than 0.765 at all points.

3. Results

3.1. Structure and electronic states of C_{60}(OH)

The optimized structure of C_{60}(OH) is illustrated in Figure 1 (upper). The C-OH and O-H distances are calculated to be 1.435 and 0.972 Å, respectively. The O-H distance of the free OH radical is 0.983 Å, indicating that the O-H bond is shortened by the addition to the surface of C_{60}. An expanded view around C-OH binding site is illustrated in Figure 1 (lower). The notation of C_0 means the carbon atom binding to the OH radical, and those of C_1, C_2, and C_3 mean the neighbor carbon atoms of C_0.

The average of C_0-C_n (n=1-3 distances of C_{60}(OH) are calculated to be 1.543 Å, which is 0.11 Å longer than that of C_{60} (1.435 Å). The average of C_n-C_0-C_m angle (*n* and *m*=1-3) of C_{60}(OH) is 106.9°, which is 13.0° smaller than that of C_{60}. The spin densities on C_0, C_1, C_1', C_2 and C_3 atoms are 0.04, 0.06, 0.46, -0.14, and 0.24, respectively. This result indicates that spin density from the OH radical is widely distributed around the carbon atom (C_0).

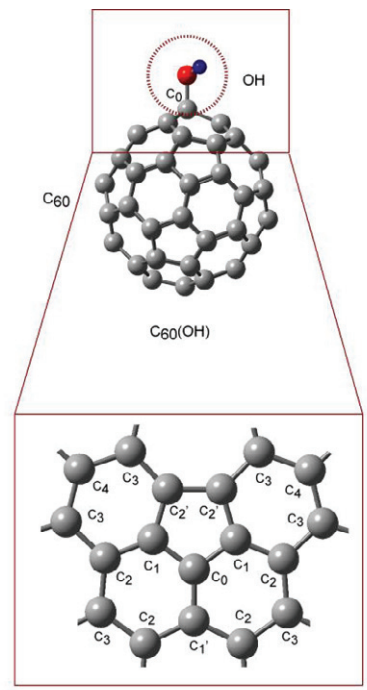

Figure 1. Optimized structure of C_{60}(OH) calculated at the B3LYP/6-311G(d,p) level (upper) and expanded view around OH addition site (lower). The OH radical is added to C_0 carbon atom.

3.2. Interaction of C_{60} with the OH radical

Potential energy curves are plotted in Figure 2 (upper) as a function of R(C-OH). Zero level of energy corresponding to total energy C_{60} + OH at the dissociation limit. At intermolecular separation of R(C-OH)=3.0 Å, the energy is -1.4 kcal/mol relative to the dissociation limit. The shape of potential energy curve shows that the interaction of OH radical with C_{60} is attractive in whole region and the energy is minimized at R(C-OH)=1.60 Å (the energy is -12.1 kcal/mol relative to dissociation limit). Next, the structure of C_{60}(OH) at the minimum point is fully optimized at the B3LYP/6-31G(d) level. The energy is stabilized to -36.4 kcal/mol and the bond distance is changed from 1.60 to 1.435 Å after the geometry optimization. The dot line indicates a schematic potential energy curve when the geometries are optimized as a function of R(C-OH). The shape of potential energy curve indicates that the addition of the OH radical takes place without potential barrier. The binding energy is 36.4 kcal/mol.

To check the existence of minimum point, the M06/6-31G(d) calculation was carried out for the potential energy curve. The M06 calculation gives the similar curve, although the binding energy of M06 is slightly larger than that of B3LYP.

The spin densities on the oxygen and hydrogen atoms are plotted as a function of R(C-OH) in Figure 2 (lower). At the dissociation limit (C_{60} + OH), the spin densities on the oxygen and hydrogen atoms are 1.03 and -0.03, respectively. The spin density of the oxygen atom decreases monotonically as OH approached to C_{60}. For example, the values on the oxygen atom at 3.0, 2.5, and 2.0 Å are 0.99, 0.90, and 0.60, respectively. At the minimum energy point, the spin density on the oxygen atom is 0.10. The spin density of the oxygen atom is changed to 0.04 after the geometry optimization, indicating that almost all spin density of OH is transferred into C_{60} at the equilibrium point. Thus, the spin density on the oxygen atom is drastically varied as a function of distance of OH from C_{60}. On the other hand, the spin density on the hydrogen atom is close to zero at all points.

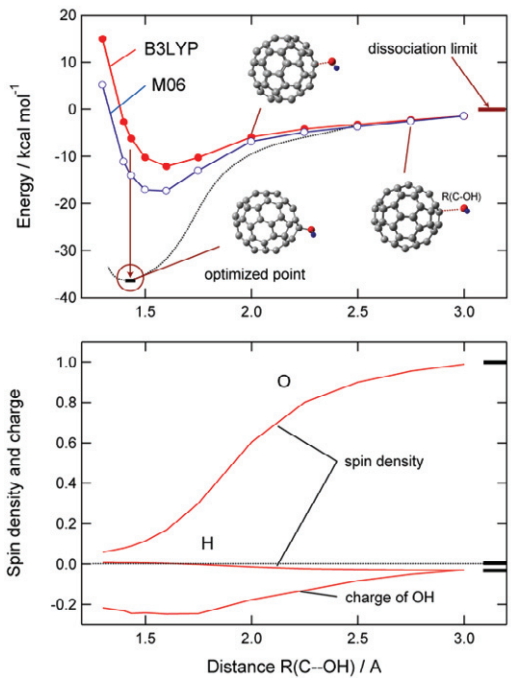

Figure 2. Potential energy curve plotted as a function of distance of R(C-OH), carbon of C_{60} and oxygen of OH, calculated at the UB3LYP/6-31G(d) and M06/6-31G(d) levels (upper). Atomic spin densities on oxygen and hydrogen atoms of OH radical, and natural atomic charge on OH radical (lower).

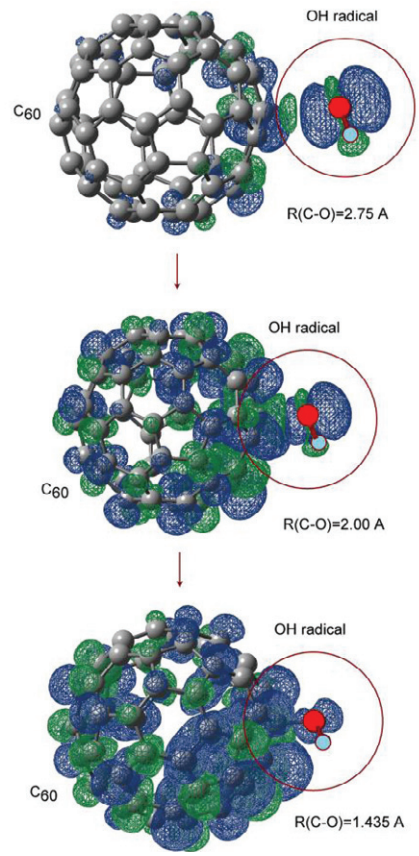

Figure 3. Spacial distribution of spin densities on C_{60}(OH). The positions of OH radical are R=(C-OH)= 2.75, 2.00, and 1.435 Å. Calculation was carried out at UB3LYP/6-31G(d) level.

The spacial distributions of spin density are illustrated in Figure 3. At a long separation, the spin density is located only in the OH radical. The spin is delocalized over the C_{60} and OH radical around r(C--OH)=2.0 Å. The spin is mainly located on the C_{60} at the equilibrium point.

For comparison, the interaction hydroxyl ion (OH^-) and C_{60} is investigated. The binding energy of OH^- to C_{60} is calculated to be 103.4 kcal/mol. The total energy of $C_{60}(OH^-)$ is 2.83 eV stable in energy than that of neutral radical $C_{60}(OH)$. This stabilization is due to the fact that electron affinity of C_{60} is positive. Therefore, addition of OH^- ion to C_{60} is highly exothermic.

3.3. Excitation energies of C_{60} and $C_{60}(OH)$

The excitation energies of C_{60} and $C_{60}(OH)$ were calculated by means of TD-DFT(UB3LYP/6-31G(d)) method. The first and second excitation energies of C_{60} are calculated to be 2.10 and 2.11 eV, respectively. When the OH radical is added to C_{60}, the energies are changed to 1.26 eV (1^{st}) and 1.32 eV (2^{nd}). This result strongly indicates that the band gap of C_{60} decreases drastically due to the addition of OH radical. This is due to the fact that new defect level is formed by the addition of OH radical.

3.4. Basis set dependence on the structure and energetics

In the present calculations, we used a standard 6-31G(d) basis set throughout. To check the basis set dependency on the energetics, the calculations of C_{60} and $C_{60}(OH)$ were carried out with a more flexible basis set, 6-311G(d,p). The geometry optimization of $C_{60}(OH)$ showed that the bond lengths of O-H and C-OH are 0.965 and 1.433 A, respectively. The binding energy of OH radical to C_{60} is 35.2 kcal/mol (6-311G(d,p) basis set), which is comparable to 34.6 kcal/mol (6-31G(d) basis set). This result indicates that the B3LYP/6-31G(d) level gives reasonable structure and electronic states of C_{60} system.

4. Summary of the present study

In the present study, the interaction of OH radical with C_{60} has been investigated by means of DFT method. The OH radical can bind to the carbon atom of C_{60} and a strong C-O bond is formed. The binding energy is calculated to be 36.4 kcal/mol at the B3LYP/6-31G(d) level. The potential energy curve plotted as a function of C-O distance shows that the OH radical approaches to the carbon atom without activation barrier. Also, it was found that structural change from sp^2 to sp^3-like hybridization occurs easily by the approach of OH. The unpaired electron is distributed widely over the C_{60} surface in the $C_{60}(OH)$ complex.

Acknowledgment. This work is partially supported by the SUHARA foundation. Also, H.T also acknowledges a partial support from a Grant-in-Aid for scientific research from The Japan Society for the Promotion of Science (JSPS) (Project No. 21550002).

References

[1] Jensen, A.W., Wilson, S.R., and Schuster, D.I., Bioorg. Med. Chem. 4 (**1996**) 767.
[2] Chiang, L.Y., Lu, F.J. and Lin, J.T. J. Chem. Soc., Chem. Commun., (**1995**) 1283.
[3] Zhu, Y.S., Sun, D.Y., Liu, G.Z., Liu, Z.Y., Zhan, R.Y., and Liu, S.Y., Chem. J. Chin. Univ. 17 (**1996**) 1127 (in Chinese).
[4] C-Y. Lu, S-D. Yao, W-Z. Lin, W-F. Wanga, N-Y. Lin, Y-P. Tong, T-W. Rong, Radiat. Phys. Chem., 53 (**1998**) 137.
[5] E.B. Zeynalov, N.S. Allen, and N.I. Salmanova, Poly. Degradat. Stabil., 94 (**2009**) 1183.
[6] Gaussian 03, Revision B.04 (Gaussian, Inc., Pittsburgh, PA, 2003).
[7] H. Tachikawa and H. Kawabata, H., J. Phys. Chem. C, 113 (**2009**) 7603.
[8] H. Tachikawa, J. Phys. Chem. C., 112 (**2008**) 10193.
[9] H. Tachikawa, J. Phys. Chem. C., 111 (**2007**) 13087.
[10] H. Tachikawa and A. Shimizu, J. Phys. Chem. B, 110 (**2006**) 20445.
[11] T. Iyama, H. Kawabata, and H. Tachikawa, Mol. Cryst. Liqud Cryst., 472 (**2007**) 697.